JOURNAL OF MATERIALS SCIENCE **40** (2005) 5483–5490

Robust design and manufacturing of ceramic laminates with controlled thermal residual stresses for enhanced toughness

NINA ORLOVSKAYA
Drexel University, 3141 Chestnut St., Philadelphia, PA 19104, USA
E-mail: orlovsk@drexel.edu

MYKOLA LUGOVY, VLADIMIR SUBBOTIN, OLEKSANDR RADCHENKO
Institute for Problems of Materials Science, 3 Krzhizhanovskii St., 03142, Kiev, Ukraine

JANE ADAMS
Army Research Laboratory, Aberdeen Proving Ground, MD 21005, USA

MUNJAL CHHEDA, JAMES SHIH
Ceradyne Inc., 3169 Redhill Ave., Costa Mesa, CA 92626, USA

JAG SANKAR, SERGEY YARMOLENKO
North Carolina A&T State University, 1601 E. Market St., Greensboro, NC 27411, USA

Boron carbide-silicon carbide ceramic composites are very promising armor materials because they are intrinsically very hard. However, their fracture toughness is not very high. Their ballistic performance could be significantly increased if the brittleness of these materials could be decreased. Here we report development of boron carbide-silicon carbide layered ceramics with controlled compressive and tensile stresses in separate layers. Such B_4C-SiC laminates with strong interfaces can provide high apparent fracture toughness and damage tolerance along with high protection capabilities.
The theory of heterogeneous layered systems was used to develop optimal design parameters allowing the evaluation and maximization of apparent fracture toughness. The layered composites were designed in a way to achieve high compressive residual stresses in thin B_4C-SiC based layers and low tensile residuals stresses in thick B_4C layers. The residual stresses were controlled by the phase composition of layers and the layers thickness. The estimated apparent fracture toughness was calculated for both three layered and nine layered composites. B_4C-30 wt%SiC/B_4C laminates were made based on the optimized design for high apparent fracture toughness. Processing of laminates involved preprocessing of powders, forming green tapes and hot pressing. Work is in progress to measure fracture toughness of laminates, as well as their strength, hardness and the ballistic performance.

1. Introduction

Ceramics offer a number of attractive properties. These include high specific stiffness, high specific strengths, low thermal conductivities, and chemical inertness in many environments. Ceramics and ceramic composites are attractive materials for use in armor systems due to low density, superior hardness, and compressive strength values relative to metals. As a result, ceramics have been subjected to a multitude of ballistic and dynamic behavior investigations [1–4]. However, the widespread usage of ceramics is currently hampered by their lack of the requisite toughness. The latest developments in ceramic composites show that the use of layered materials is perhaps the most promising method to control cracks and brittle fracture by deflection, microcracking, or internal stresses [5–7]. Laminates with strong interfaces, combined with excellent fracture toughness and damage tolerance, can potentially provide the highest ballistic performance. The way to achieve the highest possible fracture toughness is to control the level of residual stresses in the individual layers. It is also a way to increase the failure strength of ceramics by creating a layer with compressive stresses on the surface that will arrest the surface cracks and achieve higher failure stresses [8]. The layer composition, as well as the system's geometry, allows the designer to control the magnitude of the residual stresses in such a way that compressive stresses in the

0022–2461
DOI: 10.1007/s10853-005-1923-x

outer layers near the surface increase strength, flaw tolerance, fatigue strength, fracture toughness and stress corrosion cracking. In the case of symmetrical laminates, this can be done by choosing the layer compositions such that the coefficient of thermal expansion (CTE) in the odd layers is smaller than the CTE of the even ones. The changes in compressive and tensile stresses depend on the mismatch of CTE's, Young's moduli, and on the thickness ratio of layers (even/odd). However, if the compressive stresses exist only at or near the surface of ceramics and are not placed inside the material, they will not effectively hinder internal cracks and flaws [9].

Boron carbide is an important ceramic material with many useful physical and chemical properties. After cubic boron nitride, it is the hardest boron containing compound [10]. Its high melting point, high elastic modulus, large neutron capture section, low density, and chemical inertness make boron carbide a strong candidate for several high technology applications. Due to its low density and superior hardness, boron carbide is a very promising material for light-weight ballistic protection. Boron carbide exists as a stable single phase in a large homogeneity range from B_4C to $B_{10.4}C$ [11]. The most stable boron carbide structure is rhombohedral with a stoichiometry of $B_{13}C_2$, $B_{12}C_3$, and some other phases close to $B_{12}C_3$ [12, 13]. The Vickers hardness of B_4C is in the range of 32–35 GPa [14]. There is an indication that hardness of stoichiometric B_4C is the highest one in comparison with boron rich or carbon rich boron carbide compositions [15–17]. However, B_4C-based composites have a relatively low fracture toughness of 2.8–3.3 MPa·m$^{1/2}$ [18]. While high hardness is one of the very important requisite indicators for a material's ballistic potential, toughness might play an equally important role in realizing that potential. Thus, materials with both high hardness and high fracture toughness are expected to yield the best ballistic performance [1, 19]. Therefore, a significant increase in fracture toughness of boron carbide based laminates has the potential for realization of improved armor material systems.

Brittleness of boron carbide ceramic laminates can be controlled by designing the distribution of residual stresses, i.e., placing the layers with high compressive stresses into the bulk of the material. The sign and value of the bulk residual stresses have to be firmly established by theoretical prediction [20]. A significant increase in ballistic protection of B_4C based laminates may be achieved by designing high compressive stresses placed into the bulk of the materials. The goal of this research was to develop the design and processing of boron carbide-silicon carbide ceramic laminates with controlled residual stresses. In this article we demonstrate a laminate design concept by determining the prospective combination of layers, their geometry and microstructure for the B_4C/B_4C-30 wt%SiC system, as well as a laminates' manufacturing route. The apparent K_{Ic} of three layered composite was measured to be 7.42 ± 0.82 MPa·m$^{1/2}$, but the detailed report on the mechanical properties, such as Young's modulus, fracture toughness, hardness, and ballistic performance of the developed laminates will be presented elsewhere [21].

2. Thermal residual stresses and its calculation

In this work the two-component brittle layered composites with symmetric macrostructure are considered. The layers consisting of different components alternate one after another, but the external layers consist of the same component. Thus, the total number of layers N in such a composite sample is odd. The layers of the first component including two external (top) layers are designated by index 1 ($j = 1$), and the layers of the second component (internal) are designated by index 2 ($j = 2$). The number of layers designated by index 1 is $(N + 1)/2$, and the number of layers designated by index 2 is $(N - 1)/2$. The layer of each component has some constant thickness, and the layers of same component have identical thickness.

There are effective residual stresses in the layers of each component in the layered ceramic composite. During cooling, the difference in deformation, due to the different thermal expansion factors of the components, is accommodated by creep as long as the temperature is high enough. Below a certain temperature, which is called the "joining" temperature, the different components become bonded together and internal stresses appear. In each layer, the total strain after sintering is the sum of an elastic component and of a thermal component [22, 23]. The residual stresses in the case of a perfectly rigid bonding between the layers of a two-component material are [7]:

$$\sigma_{r1} = \frac{E_1' E_2' f_2 (\alpha_{T2} - \alpha_{T1}) \Delta T}{E_1' f_1 + E_2' f_2} \tag{1}$$

and

$$\sigma_{r2} = \frac{E_2' E_1' f_1 (\alpha_{T1} - \alpha_{T2}) \Delta T}{E_1' f_1 + E_2' f_2}, \tag{2}$$

where $E_j' = E_j/(1 - \nu_j)$, $f_1 = \frac{(N+1)l_1}{2w}$, $f_2 = \frac{(N-1)l_2}{2w}$, E_j and ν_j are the elastic modulus and Poisson's ratio of j-th component respectively, l_1 and l_2 are the thickness of layers of the first and second component, α_{T1} and α_{T2} are the thermal expansion coefficients (CTE) of the first and second components respectively, ΔT is the difference in temperature of joining temperature and current temperature, and w is the total thickness of the specimen.

Equations 1 and 2 give the residual stresses in layers, which have an infinitive extent. Far away from the free surface, the residual stress in the layer is uniform and biaxial. In the bulk of layers, the stress perpendicular to the layers is zero. At the free surface of the laminates, the stresses are different from the bulk stresses. Near the edges, the residual stress state is not biaxial because the edges themselves must be traction-free. Highly localized stress components perpendicular to the layer plane exist near the free surface and it decreases rapidly from the surface becoming negligible at a distance approximately on the order of the layer thickness. These stresses have a sign opposite to that of the equibiaxial stresses deep within the layer. Therefore, if the bulk stress is compressive within the material, the tensile

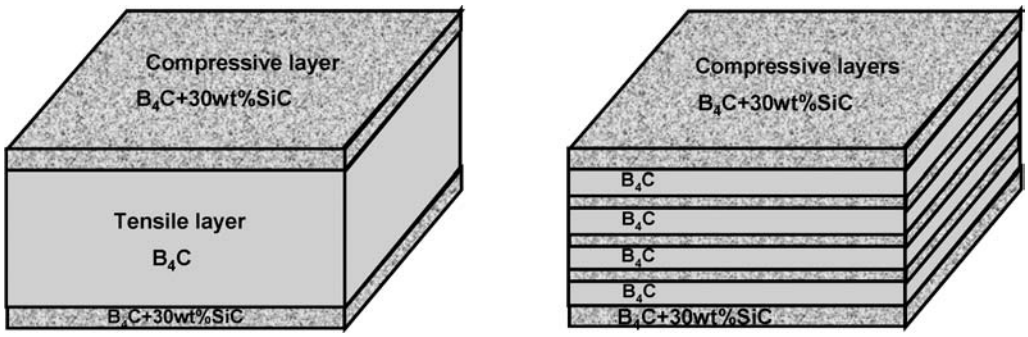

Figure 1 Schematic presentation of symmetric 3 layered and multilayered composite.

stress components appear at or near the free surface of a layer.

3. Laminate design for enhanced fracture toughness

The schematic presentation of symmetric three-layered and nine-layered composites are shown in Fig. 1. The proposed design targeted a fracture toughness increase of B_4C-SiC composites and was based on the preliminary results both from our work [24–26] and from the work of others [9, 27–30].

In case of non-homogeneous (particularly, layered) materials, so-called apparent fracture toughness should be considered. This is the fracture toughness of some effective homogeneous specimen. If we measure fracture toughness in bending, the effective sample parameters should satisfy the following conditions: (1) the specimen has to have the same dimensions as a real layered specimen; (2) the notched sample has a notch depth equal to that of the real layered specimen; (3) under the same loading conditions the specimen has to demonstrate the same load to fracture as that of the real layered specimen. Under these considerations the apparent fracture toughness is the fracture toughness calculated from a testing data of the layered sample considering this specimen as "homogeneous". Such an approach does not meet the fracture mechanics requirement of taking into account all features of stress distribution near crack tip in layered media, but it is still a useful characteristic allowing an effective contribution of such factors as residual stresses and a material inhomogeneity to be accounted for.

The compressive residual stress σ_r in the top layers of a laminate shields natural and artificial cracks in the layer. Therefore, the effective (apparent) fracture toughness of such a structure increases. The more compressive residual stress induces, the more shielding occurs. Another important factor that contributes to the apparent fracture toughness increase is a crack length a. A longer crack promotes more shielding. A maximum length of a transverse crack in a top compressive layer is limited by the layer thickness l_1. These two factors determine the apparent fracture toughness of the material.

In general, a condition of a crack growth onset is $K_a + K_r = K_c$, where $K_a = K_a(\sigma_a, a)$ is the applied stress intensity factor that can be measured, σ_a is the distribution of applied stress resulted from bending, $K_r = K_r(\sigma_r, a)$ is the stress intensity factor due to a residual stress, and K_c is the intrinsic fracture toughness of a material in the layer. If a condition of a crack growth onset is fulfilled then $K_a = K_c - K_r$ is the apparent fracture toughness. If σ_r is compressive, then $K_r < 0$ and K_a increases. The more $|\sigma_r|$, the more K_a.The more a, the more K_a.The largest value of a crack length in compressed layer is l_1. The maximum apparent fracture toughness can be obtained for such crack. Unfortunately, small cracks have K_a close to K_c.

A schematic presentation of factors that affect an apparent fracture toughness is shown in Fig. 2. Note, that the contribution of a residual stress to the maximum apparent fracture toughness is $K_r = Y(l_1/\mathrm{w})\sigma_r l_1^{1/2}$, where $Y(l_1/\mathrm{w})$ is a geometrical factor. The factor $Y(l_1/\mathrm{w})l_1^{1/2}$ increases as l_1 increases (Fig. 2a). The compressive residual stress decreases as l_1 increases. It can be calculated using Equation 1. In addition, the residual stress depends on the number of layers in the sample (Fig. 2b). The final dependences of K_a on l_1 for various numbers of layers are shown in Fig. 2c. These dependences are non-monotonic curves with a maximum that depends on a number of layers in the laminate. The labels $w/5$, $w/4$, $w/3$ and $w/2$ designate the maximum thickness of the top layer for symmetrical layered structures with 9, 7, 5 and 3 layers, respectively. It can be seen that the highest apparent fracture toughness can be obtained for the three-layer specimen. Thus, the study of the layers'

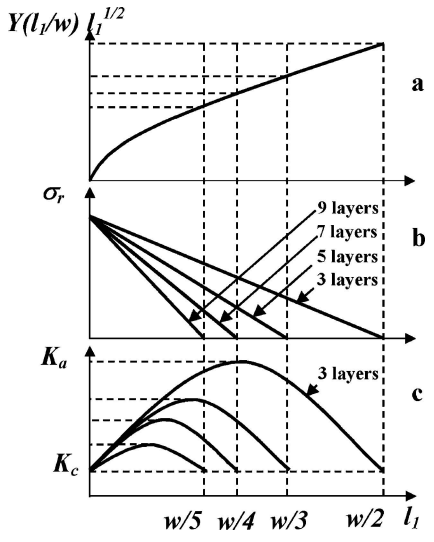

Figure 2 Factors affecting laminate design for maximum apparent fracture toughness.

relative thickness and layers' numbers reveals that the maximum crack shielding will be achieved for three-layer composites with an edge crack extending to the first interface. However, the multilayered design is also very important to meet specific ballistic requirements. It is essential during impact loading to have more barriers to arrest cracks. In our case it is the number of compressive layers. For a three-layer design there is only one such barrier that is a top compressive layer. The top layer plays a key role for the projectile defeat, however multilayered design is of further importance to stop cracks more effectively. Therefore, we designed and manufactured both three-layered and nine-layered composites in this work.

The input parameters of laminate design are the coefficients of thermal expansion, Young's moduli, Poisson's ratios, and densities of the constituents of layered composite. A very important but experimentally unknown input parameter is also ΔT – a "joining" temperature. The output parameters are layers thickness and composition. The step-by-step design technique to obtain the enhanced fracture toughness of a layered composite is as follows:

1. The compositions of layers are selected depending on a future application of the composite. Then, the relevant material constants entering the design are determined.
2. The effective coefficients of thermal expansion, an effective Young's modulus, an average density and a thickness ratio of layers are determined using the rule of mixture.
3. The next step of design is the selection of the layer's number. It can be any appropriate number depending on the required total thickness of the tile. To obtain the enhanced fracture resistance of layered composite, the factors affecting the apparent fracture toughness should be taken into account. Usually, the thickness of the thinnest possible layer is limited by the manufacturing technology. Note that a compressive layer should be thin enough to reach high level of residual stress.
4. The ratio of tensile and compressed layer thickness (thickness ratio) is determined. Any appropriate thickness ratio can be used as a first approximation.
5. Tensile layer thickness is found.
6. The calculation of residual stresses is fulfilled using (1) and (2). The total thickness of the sample is also determined at this step for a given layer's thickness ratio taking into account the selected number of layers.
7. The thickness ratio is changed after analysis of the residual stress and the total thickness of the specimen. Note that increasing ratio of tensile layer thickness to compressive layer thickness decreases tensile residual stress. However, it can result in increasing total thickness of sample.

After changing thickness ratio, the calculation is repeated. Such iterations are continued to find a unique optimal layer thickness ratio that produces the maximum possible compressive residual stress, low tensile residual stress, and required total thickness of the sample. The maximum possible apparent fracture toughness of the corresponding layered structure is also determined in all iterations as an indicative parameter of the design. The determination of the apparent K_{Ic} uses the compressive residual stress and the thickness of a top layer as a crack length at any given iteration. These two parameters (the compressive residual stress and the thickness of the top layer) have trends acting in opposite directions. A decrease in the top layer thickness can increase the residual stress in the layer, but it decreases the length of the maximum crack. Therefore, the maximum apparent fracture toughness was always used to analyze the correct thickness ratio.

4. Processing of laminates

The material systems selected for the proposed study were B_4C and B_4C-30 wt%SiC because of their promise for ballistic applications [31–33]. Table I shows the relevant material properties used in the design calculations (compiled from literature), and Tables II and III show the corresponding calculated residual stresses in the B_4C/B_4C-30 wt%SiC laminates. The maximum possible apparent fracture toughness for corresponding layered structures is also presented in the Tables II and III. The layers under tensile stress have higher CTE, and in this case they are B_4C layers. The layers under compressive stress have lower CTE; here they are B_4C-30 wt%SiC layers. A temperature $T = 2150^{\circ}C$ was used for the majority of the calculations, when residual stresses appeared in the layers upon cooling from the hot pressing temperature. There is no liquid phase present during the sintering of B_4C/B_4C-SiC ceramics [34], therefore, the hot pressing temperature was used as a "joining" temperature ΔT for calculations. It should be noted that all laminates were designed in such a way that the tensile stresses had been maintained at low values.

B_4C and α-SiC powders with a grain size of 2–5 μm were used for laminates manufacturing. B_4C-30 wt%SiC mixtures were made by ball milling the respective powders in acetone in a polyethylene bottle using B_4C milling media 48 h. The laminates were produced via rolling of tapes followed by hot pressing. The formation of a thin ceramic layer is of specific importance, as the sizes of residual stress zones (tensile and compressive) are directly connected to the thickness of layers. The advantage of rolling, as a method of green layers production, are that it allows easy thickness control, achieves high green density of the tapes, and requires a rather low amount of solvent and organic additives as compared to other methods like tape casting [35]. Additional powder refinement, giving a higher sintering reactivity, might occur due to large forces applied in the pressing zone during rolling. The modeling of rolling was recently performed that potentially

TABLE I Properties of ceramics used in the stress calculation

Composition	E (Gpa)	Poisson's ratio	CTE (10^{-6} K^{-1})
B_4C	483	0.17	5.5
SiC	411	0.16	3

TABLE II Three layered composite design. A total thickness of a tile – 10.5 mm

Composition	Thickness of Layers (μm)		σ_{comp} (MPa)	σ_{tens} (MPa)	Apparent K_{Ic} (MPam$^{1/2}$)
	B_4C-30wt%SiC	B_4C			
B_4C-30wt%SiC/B_4C	900	8700	632	131	44

TABLE III Nine layered composite design. A total thickness of a tile – 10.35 mm

Composition	Thickness of Layers (μm)		σ_{comp} (MPa)	σ_{tens} (MPa)	Apparent K_{Ic} (MPam$^{1/2}$)
	B_4C-30wt%SiC	B_4C			
B_4C-30wt%SiC/B_4C	150	2250	662	99	32

TABLE IV Some properties of the powders and green tapes after rolling

Composition	d_{50} (μm)	Additive density (g/cm^3)	Poured density of the powder	Poured density of the granulas	Green Tape	
					Relative density	Thickness (mm)
B_4C	2.5	2.52	0.111	0.095	0.71	0.45
B_4C-30wt%SiC/B_4C	1.5	2.69	0.186	0.146	0.74	0.47

allows optimizing the process of roll compaction [36]. In our case there is a challenging problem to produce thin tapes with a small amount of plasticizer and sufficient strength and elasticity to handle green layers after rolling. Crude rubber (1–3 wt%) has to be added to the mixture of powders as a plasticizer through a 3% solution in petrol. Then the powders were dried up to the 2 wt% residual amount of petrol in the mixture. After sieving powders with a 500 μm sieve, granulated powders were dried up to the 0.5 wt% residual petrol. The schematic presentation of rolling is shown in Fig. 3.

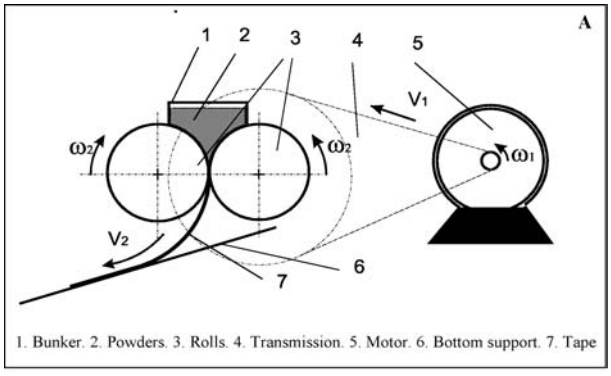

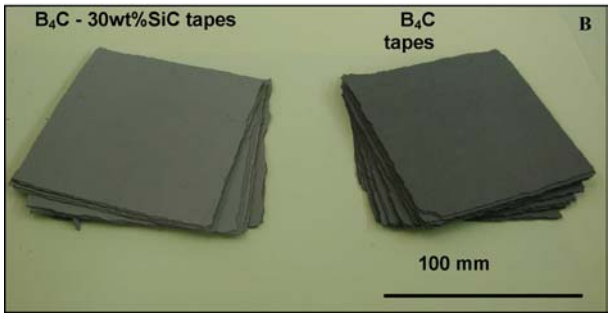

Figure 3 (A) Schematic presentation of rolling. (B) Photograph of B_4C and B_4C-30 wt%SiC rolled tapes. The thickness of an individual tape after rolling is between 0.4–0.5 mm.

Powders are continuously supplied in the bunker and further into the deformation zone in between rolls. Powders are supplied to the deformation zone due to both the gravitational force and friction between rolls and powders. The relative density of the tape (ρ_r) can be calculated from

$$\rho_r = \frac{\rho_p}{\lambda}\left(1 + \frac{\alpha^2 R}{h_s}\right) \tag{3}$$

where ρ_p is a relative powder density, λ is a drawing coefficient, α is an intake angle, and R is a roll diameter. A roll mill with 40 mm rolls was used for rolling. The velocity of rolling was in the range of 1–1.2 m/min. Working pressure was varied from 0.1 ton/cm^2 for relative density of tapes 64% to 1 ton/cm^2 for 74% density. The properties of the powders and green tapes after rolling are presented in Table IV.

Samples of ceramics were prepared by hot pressing of the rolled tapes stacked together. The hot pressing conditions were as follows: (a) a heating rate was 100°C/min; (b) a hot pressing temperature was kept at 2150°C during hot pressing of a majority of the tiles, and some hot pressing was done at 2200°C to ensure that fully dense materials were obtained; (c) a pressure was kept at the level of 30 MPa; and (d) a dwell time at hot pressing temperature was 50–60 min. Graphite dies were used for the hot pressing of laminates with graphite surfaces coated by BN layer in order to prevent a direct contact between graphite and ceramic material. 90 × 90 × 10 mm tiles were produced as a result of hot pressing. Dense (97–100% of density) laminate samples were obtained.

5. Microstructure of laminates

During hot pressing of laminates the shrinkage of the individual layers occurred, and their thickness become 0.15 mm after hot pressing. The interfaces between

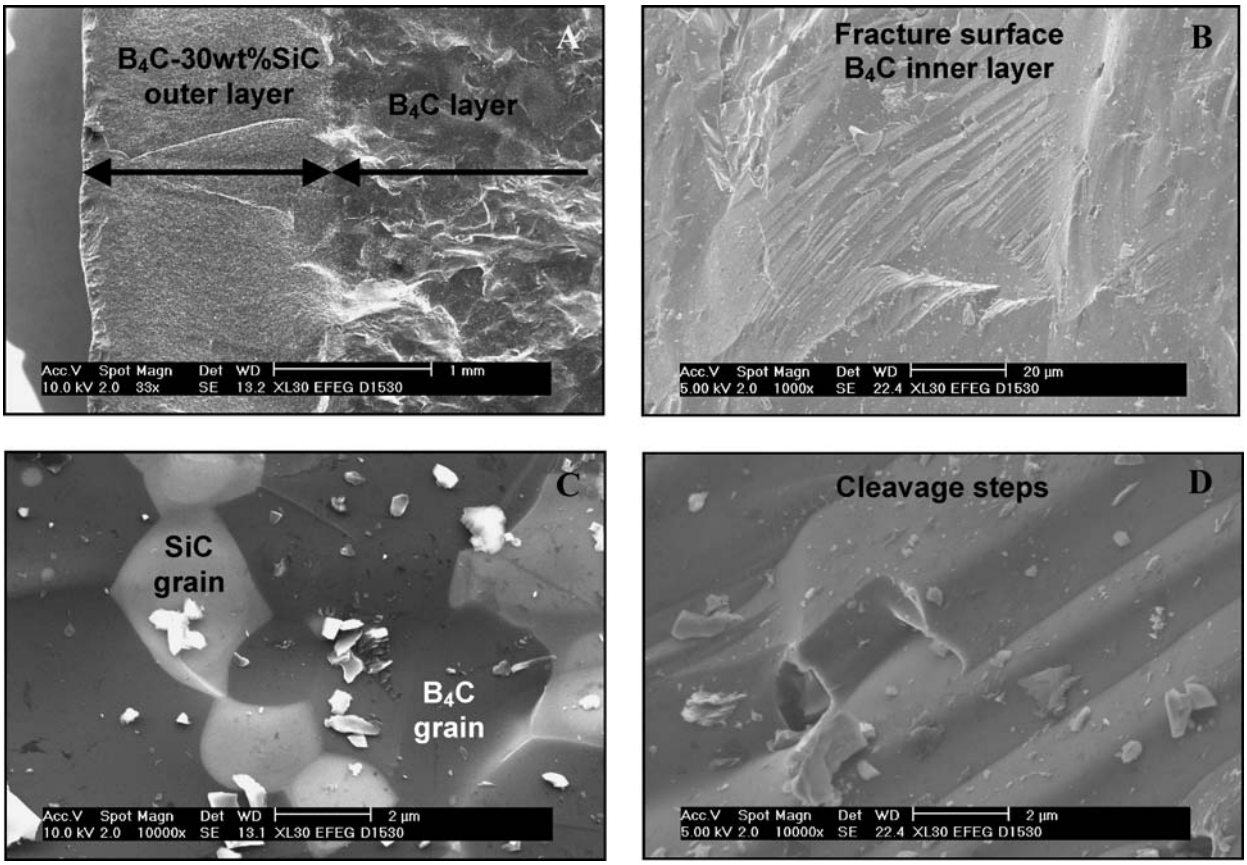

Figure 4 Fracture surface of a three layered tile. (A) An interface between B_4C-30 wt%SiC outer layer and pure B_4C inner layer; (B) A fracture surface of B_4C layer; (C) A fracture surface of B_4C-30 wt%SiC; (D) Cleavage steps on the B_4C fracture surface.

individual layers of the same composition completely disappeared and only the interface between B_4C-30 wt%SiC and B_4C layers could be distinguished.

A fracture surface of a three-layer tile hot pressed at 2200°C for 1 h is shown in Fig. 4. The layered composite demonstrates typical brittle fracture. The interface between the B_4C-30 wt%SiC outer layer and the pure B_4C inner layer is shown in Fig. 4a. The fracture surface of the B_4C layer is presented in Fig. 4b. Fig. 4c shows the fracture surface of the B_4C-30 wt%SiC layer. The cleavage steps on the B_4C fracture surface are presented in Fig. 4d. Such cleavage mode plays an important role both in fracture and in the fragmentation event during ballistic impact [37].

As one can see from Fig. 4, the B_4C grain size in B_4C-30 wt%SiC layers was in the range of 4–6 μm, SiC grain size was in the range of 2–5 μm. B_4C grain size in pure B_4C layers could not be calculated because of a pure transgranular fracture mode with no grains or grain boundaries revealed after fracture. Significant grain growth of boron carbide is expected during hot pressing at 2200°C. However, in B_4C-30 wt%SiC layers, the existence of the SiC phase prevented the exaggerated grain growth and the grain size distribution was homogeneous. Tiles hot pressed at 2200°C for 1 h were fully dense. Tiles hot pressed at 2150°C for 30 or 45 min contained some amount of porosity (2–5%) that was concentrated along the interfaces and mostly in pure B_4C layers. Such porosity could be detrimental for material hardness, affecting Young's modulus and density, thus significantly lowering the ballistic performance of the laminates. As a result of the hardness and Young's modulus decrease, the mterial with a residual porosity more then 2% cannot be considered as a candidate for ballistic protection.

6. What residual stresses can do with a laminate

During the assembly of one 100 × 100 × 12 mm multilayered tile, inner thin B_4C-30 wt%SiC layers were mistakenly replaced with pure B_4C thin layers. As a result, instead of a multilayered tile, 3 layered laminate was produced. The parameters of this 3-layered tile, including a thickness of layers and calculated stresses are presented in Table V. The outer B_4C-30 wt%SiC layers had their thickness of 1650 μm, and the thick B_4C layer had a thickness of 9000 μm. For such design the level of residual tensile stress has been raised to 210 MPa after cooling from $T_{HP} = 2200$°C. Such a high residual tensile stress leads to a complete fracture of the tile during decompression of the graphite die to separate a tile after hot pressing (Fig. 5). The failure apparently started from the tile edges with cracks propagated further into the tile body.

This example shows the importance of determination of a critical value of the tensile stress in a layer. Certain difficulties exist to find this critical value. One of the problems is that the mechanical properties of an individual layer can significantly deviate from the ones of a corresponding bulk material. We can easily calculate the critical tensile stress if intrinsic fracture toughness of layer and size of critical flaw inside the layer are

TABLE V Three layered composite design. A total thickness of a tile – 12.30 mm

	Thickness of Layers (μm)			
Composition	B_4C-30wt%SiC	B_4C	σ_{comp} (MPa)	σ_{tens} (MPa)
B_4C-30wt%SiC/B_4C	1650	9000	573	210

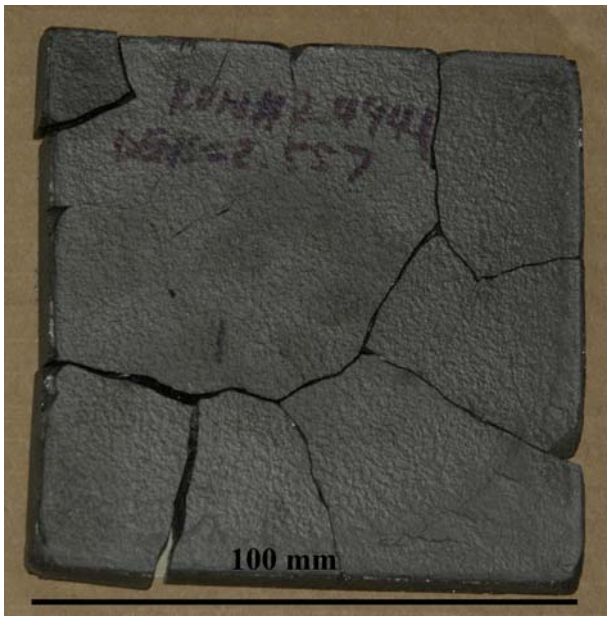

Figure 5 Photograph of fractured 3 layered B_4C-30 wt%SiC /B_4C tile hot pressed at 2200°C.

known but the critical defect in the layer usually cannot be identified. There is a possibility to determine the stress for crack tunneling in the tensile layer [38]. Such stress depends only on the intrinsic fracture toughness and the layer thickness. Such transverse cracking of a tensile layer is not possible if the tensile residual stress has a lower value than the stress for crack tunneling. Therefore, some empirical value is used as a critical tensile stress. Such approach, in fact, is also rather successful to eliminate cracking in laminates.

7. Conclusions

This research represents a first step in laminate ceramics development that should provide sufficient ballistic protection. Boron carbide-silicon carbide ceramics have been used in the design and manufacturing of three layered and multilayered composite with strong interfaces for enhanced fracture toughness. The model of heterogeneous layered system was used to develop optimal design parameters. As a result, laminates with calculated high compressive residual stresses (up to 650 MPa) and low tensile residual stresses (below 150 MPa) were developed. The feasibility of manufacturing laminate composite systems with enhanced toughness by incorporation of thin layers with high compressive stresses in the ceramics was demonstrated. Both three-layered and nine-layered B_4C-30 wt%SiC/B_4C composites were manufactured using roll-forming and hot pressing techniques. Work is currently in progress to study the mechanical properties, such as fracture toughness, strength, hardness, as well as ballistic performance of developed B_4C-30 wt%SiC/B_4C ceramic laminates. The results of this study are likely to find practical applications in the field of ballistic protection and mechanical behavior of advanced ceramic composites.

Acknowledgement

This work was supported by AFOSR, the project no. F49620-02-0340 and by the European Commission, the project ICA2-CT-2000-10020, Copernicus—2 Program. This work was also partly performed at the Army Center for Nanoscience and Nanomaterials, North Carolina A&T State University.

References

1. J. S. STERNBERG, *J. Appl. Phys.* **69** (1989) 3417.
2. D. A. SHOCKEY, A. H. MARCHAND, S. R. SAGGS, G. E. CORT, M. W. BUZKETT and R. PARKER, *Int. J. Impact Eng.* **9** (1990) 263.
3. G. R. JOHNSON and T. J. HOLMQUIST, *J. Appl. Phys.* **85** (1999) 8060.
4. H. D. ESPINOSA, N. S. BRAR, G. YUAN, Y. XU and V. ARRIETA, *Int. J. Sol. Struct.* **37** (2000) 4893.
5. W. J. CLEGG, *Science* **286** (1999) 1097.
6. M. LUGOVY, N. ORLOVSKAYA, K. BERROTH and J. KUEBLER, *Comp. Sci. Technol.* **59** (1999) 283.
7. *Idem.*, *ibid.* **59** (1999) 1429.
8. P. HONEYMAN-COLVIN and F. F. LANGE, *J. Am. Ceram. Soc.* **79** (1996) 1810.
9. M. P. RAO, A. J. SANCHEZ-HERENCIA, G. E. BELTZ, R. M. MCMEEKING and F. F. LANGE, *Science* **286** (1999) 102.
10. I. J. MCCOLM, "Ceramic Hardness" (Plenum Press, New York, 1990).
11. K. A. SCHWETZ and A. LIPP, "Ulmann's Encyclopedia of Industrial Chemistry", A4, VCH, (1981), 295.
12. E. AMBERGER, W. STUMPF and K.-C.BUSCHBECK, "Handbook of Inorganic Chemistry", 8th ed. (Springer-Verlag, Berlin, 1981).
13. D. M. BYLANDER and L. KLEIMAN, *Phys. Rev. B* **43** (1991) 1487.
14. F. THEVENOT, *J. Eur. Ceram. Soc.* **6** (1990) 205.
15. B. CHAMPAGNE and R. ANGERS, *J. Am. Ceram. Soc.* **62** (1979) 149.
16. K. NIIHARA, A. NAKAHIRA and T. HIRAI, *ibid.* **67** (1984) C13.
17. F. TREVENOT, in "Properties of Ceramics", edited by G. de With, R. A. Terpstra, and R. Metselaar. (Elsevier Appl. Sci., London and New York, 1989).
18. H. LEE and R. SPEYER, *J. Am. Ceram. Soc.* **85** (2002) 1291.
19. M. L. WILKENS, *Int. J. Eng. Sci.* **16** (1978) 793.
20. C. A. FOLSOM, F. W. ZOK and F. LANGE, *J. Am. Ceram. Soc.* **77** (1994) 689.
21. N. ORLOVSKAYA, M. LUGOVY and J. KUEBLER, Mechanical performance of 3 layered B_4C-SiC ceramic composites, unpublished results.
22. S. HO, C. HILLMAN, F. F. LANGE and Z. SUO, *J. Am. Ceram. Soc*. **78** (1995) 2353.
23. T. CHARTIER, D. MERLE and J. L. BESSON, *J. Europ. Certam. Soc.* **16** (1995) 101.

24. V. YAROSHENKO, N. ORLOVSKAYA, M. -A. EINARSRUD and V. KOVYLAYEV, in Proceedings of NATO ARW "Multilayered and Fibre-Reinforced Composites: Problems and Prospects", edited by Y. Haddad, (Kluwer, Dordrecht, 1998).
25. N. ORLOVSKAYA, J. KUEBLER, M. LUGOVY and V. SUBBOTIN, *J. Am. Ceram. Soc.* submitted, 2002.
26. M. LUGOVY, N. ORLOVSKAYA, V. SLYUNYAYEV, G. GOGOTSI, J. KUEBLER and A. SANCHEZ-HERENCIA, *Compo. Sci. Technol.* **62** (2002) 819.
27. M. OECHSNER, C. HILLMAN and F. LANGE, *J. Am. Ceram. Soc.* **79** (1996) 1834.
28. D. GREEN, P. CAI and G. MESSING, *J. Europ. Ceram. Soc.* **19** (1999) 2511.
29. R. LAKSHMINARAYANAN, D. K. SHETTY and R. A. CUTLER, *J. Am. Ceram. Soc.* **79** (1996) 79.
30. A. BLATTNER, R. LAKSHMINARAYANAN and D. K. SHETTY, *Eng. Frac. Mech.* **68** (2001) 1.
31. C. J. SHIH, M. A. MEYERS, V. F. NESTERENKO and S. J. CHEN, *Acta. Mater.* **48** (2000) 2399.
32. D. L. ORPHAL, R. R. FRANZEN, A. C. CHARTERS, T. L. MENNA and A. J. PIEKUTOWSKI, *Int. J. Impact Eng.* **19** (1997) 15.
33. D. L. ORPHAL and R. R. FRANZEN, *ibid.* **19** (1997) 1.
34. P. S. KISLYI, M. A. KUZENKOVA, N. I. BONDARUK and B. L. GRABCHUK, "Boron Carbide" (Naukova Dumka, Kiev, 1988) (in Russian).
35. T. P. HYATT, *Ceram. Eng. Sci. Proc.* **16** 71.
36. R. T. DEC, A. ZAVALIANGOS and J. C. CUNNINGHAM, *Powder Technol.* **130** (2003) 265.
37. M. CHEN, J. W. MCCAULEY and K. J. HEMKER, *Science* **299** (2003) 1563.
38. S. HO and Z. SUO, *J. Appl. Mech.* **60** (1993) 890.

Received 2 February 2004
and accepted 16 February 2005